

Effect of iron dissolution on cloud chemistry: from laboratory measurements to model results

Laurent Deguillaume^{1,2}, Karine V. Desboeufs³, Maud Leriche⁴, Yoann Long^{1,2}, Nadine Chaumerliac^{1,2}

¹ Clermont Université, Université Blaise Pascal, OPGC, Laboratoire de Météorologie Physique, F-63000 CLERMONT-FERRAND, France

² CNRS, UMR 6016, LaMP, F-63177 CLERMONT-FERRAND, France

³ Laboratoire Inter-Universitaire des Systèmes Atmosphériques, CNRS, Universités Paris 7 et Paris 12, CNRS, UMR 7583, CRETEIL, France

⁴ Laboratoire d'Aérodynamique, Université Paul Sabatier, CNRS, TOULOUSE, France

ABSTRACT

This study investigates the influence of iron dissolution from aerosol particles on cloud chemistry and presents improvements in modeling of the associated multiphase processes. Iron redox species are important pollutants; they are very reactive in clouds especially through their interactions with H_xO_y compounds. Solid phase iron is transferred into the aqueous-phase by dissolution. The rate of dissolution of iron drives its concentration in the solid and aqueous-phases and has been determined in laboratory based on dissolution experiments using an urban particles standard. The parameterization of the iron dissolution rate and iron redox speciation as a function of time, stemming from the experimental data, was implemented in the cloud chemistry model M2C2 (Model of Multiphase Cloud Chemistry). A continental cloud event with simplified microphysical properties was simulated. Two simulations were performed: (1) using a predefined fixed iron content, and (2) using iron content values evolving temporally resulting from the dissolution parameterization. Numerical results show that the iron speciation (i.e. the partitioning between iron oxidation states) is driven by the chemical reactivity and not by dissolution. The oxidative capacity of the atmospheric cloud water decreases when dissolution is included in the model. The flux of OH radicals produced is positively correlated to the concentration of iron present that continuously increases with time throughout the simulation. Thus, ignoring the iron dissolution kinetics results in overestimations of net OH production, by factors of 1.7 and 1.2 after 5 minutes and 2 hours of the simulation, respectively. This study concludes that the consideration of the dissolution process is potentially important in estimating radical concentrations and hence cloud oxidative capacity.

Keywords:

Cloud chemistry

Modeling tools

Iron

Radicals

Aerosol mass transfer

Dissolution

Article History:

Received: 31 March 2010

Revised: 22 June 2010

Accepted: 29 June 2010

Corresponding Author:

Laurent Deguillaume

Tel: +33-473407359

Fax: +33-473405136

E-mail: L.Deguillaume@opgc.univ-bpclermont.fr

© Author(s) 2010. This work is distributed under the Creative Commons Attribution 3.0 License.

doi: 10.5094/APR.2010.029

1. Introduction

Chemical and physical processes occurring in cloud systems significantly modify the transport, vertical redistribution, chemical transformation, and removal of chemical species from the atmosphere, and hence impact on the lifetime of both aerosol particles and trace gases (Fowler et al., 2009). Moreover, the chemical composition of aqueous atmospheric water is critical in estimating the atmospheric fluxes of nutrients essential to phytoplankton growth via wet deposition (Jickells et al., 2005). The main processes driving the chemical composition of cloud droplets are (1) the microphysical processes that drives cloud formation (nucleation) and evolution (evaporation, condensation, collision, coalescence), (2) the chemical composition and concentration of aerosols dissolved in the droplets from nucleation and impaction scavenging, (3) the transfer of soluble species at the air/water interface during the cloud lifetime and (4) the complex chemical reactivity in the liquid phase (Herrmann, 2003; Herrmann et al., 2005). In clouds, the aqueous-phase reactions are usually faster than the equivalent reactions in the gas-phase. The reactivities of ionic species are of primary importance and the actinic flux leading to photochemical processes inside the cloud droplets are much stronger than in interstitial air.

Modeling studies have attempted to understand the overall role of cloud chemistry in global climate studies, but our

knowledge of the detailed cloud chemistry is still incomplete. Process models make it possible to simulate complex interactions between microphysical, chemical, radiative, and dynamic processes. These detailed air parcel models have been used to simulate the particle evolution along pre-determined trajectories in several studies (e.g. von Glasow et al., 2003; Medina and Nenes, 2004; Tilgner et al., 2005; Gelencser and Varga, 2005; Wolke et al., 2005; Barth, 2006; Leriche et al., 2007; Sehili et al., 2007; Ervens et al., 2008). When considering aerosol particles, they offer the possibility to de-couple contributions from gaseous and particulate-phase to the solute composition and concentration in cloud samples. So, they offer the possibility to estimate the phase partitioning of chemical compounds between gas and condensed phases and to discuss the particulate and gaseous contributions to the observed ionic concentration in cloud droplets. Furthermore, these models also provide very useful tools to focus on individual processes that can be studied in more detail before their incorporation into multidimensional atmospheric codes.

In this context, transition metal ion (TMI) chemistry in clouds is still subject to large uncertainties (Deguillaume et al., 2005a; Deguillaume et al., 2005b; Alexander et al., 2009). Transition metals in the atmospheric particulate-phase are initially transferred into liquid phase from aerosol particles by dissolution processes. The major atmospheric chemical effects of transition metals take place through homogeneous aqueous-phase

chemistry in cloud droplets, and raindrops where they undergo catalytic and photo-catalytic cycles. TMI are involved in numerous chemical reactions, such as the oxidation of S(IV), the budget of H_2O_2 , and the formation of free radicals (OH , HO_2/O_2) (Deguillaume et al., 2004). Among transition metals, iron is the most abundant and the most reactive in the atmospheric liquid phase with a crucial role on the aqueous HO_x chemistry. The oxidation state of iron alters its reactivity in solution and it is highly variable depending on the solution's pH, the concentration of oxidants, the concentration of complexing agents and of the intensity of the actinic flux (Erel et al., 1993; Sinner et al., 1994; Ozsoy and Saydam, 2001; Parazols et al., 2006). In chemical models, large uncertainties arise from estimates of trace metals concentrations and redox speciation in tropospheric waters. Currently, the mass transfer rate between the atmospheric particulate and aqueous-phases is poorly studied. Consequently, atmospheric chemistry models have not yet considered the dissolution kinetics of iron and rely on empirical methods to initialize its concentration in cloud droplets based on measured dissolved trace metal concentrations in cloud and rainwater.

However, dissolution studies show that the release of iron from aerosol particles into aqueous-phase lasts from several minutes up to hours and appears to be an initial rapid release of iron, followed by a slow and sustained release (Spokes and Jickells, 1996; Hoffmann et al., 1997; Desboeufs et al., 1999; Mackie et al., 2005). Several studies on aerosol dissolution have shown that the release of iron in rainwater is dependent on a number of factors, the most important of which are the droplet pH and the physico-chemical nature of the particles that evolves during the aerosol aging in the atmosphere (Chester et al., 1993; Spokes et al., 1994; Zuo, 1995; Desboeufs et al., 1999; Desboeufs et al., 2001; Hand et al., 2004; Desboeufs et al., 2005). Consequently, on the scale of droplet lifetimes, dissolved iron concentrations increase continuously.

In this paper, we discuss the effect of the iron dissolution on cloud chemistry using a modeling strategy based upon laboratory experiments. In the first section the experimental approach used to determine the rate constants for the dissolution of iron in cloud droplets is presented. The experimentally determined rate constants are then implemented in the M2C2 model (Model of Multiphase Cloud Chemistry) which incorporates explicit treatment of multiphase cloud chemistry. Using this method, the temporal evolution of the dissolved iron concentration in cloud water was realistically modeled during the simulated cloud event. The results obtained using the “traditional” scenario with fixed initial iron content and with the consideration of the dissolution process were compared, and discussed in terms of iron redox speciation and effects on H_xO_y chemistry.

2. Dissolution of Iron: from the Laboratory Experiment to the Numerical Model

2.1. Leaching experiment

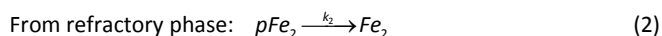
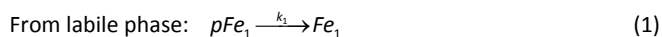
To investigate the iron dissolution process into atmospheric waters, dissolution experiments were carried out using Urban Particulate matter (UP, diameter 30 nm to 10 μm) provided by NIST as a standard reference material (SRM 1648). The physico-chemical characteristics of particulate matter are described in detail in previous studies (Desboeufs et al., 2003b; Desboeufs et al., 2005). The urban particulate matter is a mixture of anthropogenic combustion particles (fly-ash and soot) and natural material (terrestrial dust, gypsum). The total iron mass content is 3.91% and is the predominant metal in UP. Microscopic observations coupled with EDX (energy dispersive X-ray spectrometry) showed that iron is contained both in aluminosilicated mineral and combustion particles.

Dissolution experiments were conducted using an open flow reactor at ambient temperature based on the protocol detailed in Desboeufs et al. (1999). The reactor allows the levels of dissolved species to be maintained below saturation in order to exclusively follow dissolution process without interference from secondary precipitation reactions. In this system, particles (20 mg) were leached by aqueous solution (2 L), in order to obtain a typical ambient particulate concentration (10 mg L^{-1}) for atmospheric waters (Ridame and Guieu, 2002). The dissolved species, i.e. passing through a 0.2 μm NucleporeTM membrane filter, were sampled in the outflow. The inlet solution simulated artificial atmospheric water by adding Suprapur sulfuric acid (H_2SO_4) in MilliQ water. The pH was fixed at 4.7, median pH in the atmospheric waters (Li and Aneja, 1992). About 30 mL of the outlet solution, containing dissolved trace metals from particulate matter, was sampled every 2 minutes during the first 30 minutes of leaching then at 45, 60, 90 and 120 minutes. Experiments were carried out in triplicate. Dissolved iron concentrations were measured by Atomic Emission Spectrometry coupled with Plasma (ICP-AES) (Desboeufs et al., 2003a). From the dissolved iron concentrations the dissolution rate of iron was determined at each time step by using the rate equation for an open reactor given in Desboeufs et al. (1999). The redox speciation of dissolved iron was also determined for one experiment based on the method described in previous experiments (Sofikitis et al., 2004; Journet et al., 2007).

2.2. Kinetic data extrapolated from dissolution experiments

The temporal evolution of the iron dissolution rate during the experiment described above is illustrated in Figure 1a and 1b. Iron dissolution rates are observed to decrease with time: the dissolution rate of iron is initially high and decreases rapidly for first 10 minutes, then it decreases at slower rates to reach values around $10^{-11} \text{ mol L}^{-1} \text{ s}^{-1}$. This is the typical behavior for metal dissolution from aerosol (Hoffmann et al., 1997; Nimmo et al., 1998; Desboeufs et al., 1999; Biscombe et al., 2004; Desboeufs et al., 2005). It has been hypothesized that the initial fast dissolution rate is due to the release of kinetically labile iron at the mineral surface and the slow dissolution rate is associated with the release of refractory iron once all the labile iron has been depleted (Stumm and Morgan, 1996; Desboeufs et al., 1999). Consequently, the dissolution process is only dependent on the iron content which can be dissolved from labile and refractory iron phases.

The release of iron from UP can be described by two simultaneous dissolution reactions, corresponding to the transfer of iron from both labile and refractory aerosol fraction ($p\text{Fe}_1$ and $p\text{Fe}_2$ respectively) into water:



For each phase, the rate of iron dissolution is proportional to the concentration of labile or refractory iron and can be described by a first order-rate law. If $p\text{Fe}_1$ is the labile fraction of iron from the solid and Fe_1 the dissolved fraction of iron from the labile phase at time t during the experiment, the first order-rate law in open reactor for dissolution reaction is given by:

$$R_1 = \frac{d[\text{Fe}_1]}{dt} = k_1 ([p\text{Fe}_1] - [\text{Fe}_1]) \quad (3)$$

where $[p\text{Fe}_1] - [\text{Fe}_1]$ represents the remaining labile fraction of iron.

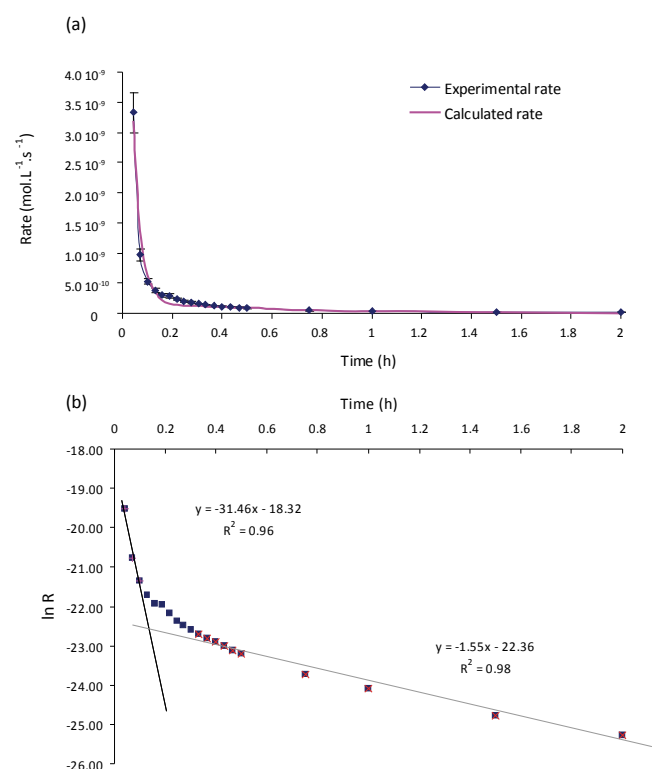


Figure 1. In blue: Experimental iron dissolution rate as a function of leaching time for urban particles; In red: Calculated iron dissolution rate (a). Linear slope-intercept form of $\ln R$ as a function of time for labile iron (black line) and refractory iron (grey line) (b).

Since $[Fe_1]=0$ at $t=0$, the integration of (E-1) gives:

$$([pFe_1] - [Fe_1]) = [pFe_1] \cdot e^{-k_1 t} \quad (4)$$

The dissolution rate is:

$$R_1 = k_1 [pFe_1] \cdot e^{-k_1 t} \text{ and } \ln(R_1) = \ln(k_1 [pFe_1]) - k_1 t \quad (5)$$

In the same way, for the refractory phase, the dissolution rate is:

$$R_2 = k_2 [pFe_2] \cdot e^{-k_2 t} \text{ and } \ln(R_2) = \ln(k_2 [pFe_2]) - k_2 t \quad (6)$$

In plotting $\ln(R)$ as a function of time, two linear regressions are identified which enable the values of the dissolution kinetic constants (k_1 , k_2) to be determined from y-intercept and labile and refractory fraction (pFe_1 and pFe_2) from slope for the two simultaneous dissolution reactions (Figure 1 and Table 1). Consequently, the total iron dissolution rate can be expressed as the sum of two dissolution rates:

$$R = k_1 [pFe_1] \cdot e^{-k_1 t} + k_2 [pFe_2] \cdot e^{-k_2 t} \quad (7)$$

The dissolution rate of iron from UP derived from the experimental data can then be implemented in the cloud chemistry model M2C2 in order to estimate the variation of dissolved iron due to the release of iron by UP during a cloud lifetime.

Table 1. Deduced rate constants and concentration of iron for the two linear steps of dissolution of iron from UP based on Figure 1b and redox speciation deduced from results presented in Figure 2

	First linear step	Second linear step
Kinetic constant (s^{-1})	$k_1 = 8.74 \times 10^{-3}$	$k_2 = 4.23 \times 10^{-4}$
Labile and refractory iron concentrations (mol L^{-1})	$[pFe_1] = 1.27 \times 10^{-6}$	$[pFe_2] = 4.39 \times 10^{-7}$
Dissolved iron redox speciation	$[Fe_{(II)}] = 0.8 [Fe_1]$ $[Fe_{(III)}] = 0.2 [Fe_1]$	$[Fe_{(II)}] = 0.5 [Fe_2]$ $[Fe_{(III)}] = 0.5 [Fe_2]$

2.3. Redox iron speciation from dissolution experiments

The redox speciation of the dissolved iron measured during the dissolution experiments on the UP are presented in the Figure 2. Results indicate that Fe(II) represents 80% of the initial dissolved iron, meaning that the dissolved iron from labile fraction is mainly Fe(II). At the end of dissolution experiment, when the dissolution from refractory phase predominates, the Fe(II) fraction is 50% and hence Fe(II) and Fe(III) are dissolved in the same proportion. This result confirms the fact that Fe(II) is generally more soluble than Fe(III), and is in agreement with previous observations (Majestic et al., 2007) showing an increase of dissolved Fe(II) concentrations with the increase of urban particles in their aerosol samples. Thus dissolved Fe(II) fractions of 80% and 50% from the labile and refractory phases respectively, have been considered in the cloud chemistry model M2C2 for the modeling part of the study (Table 1).

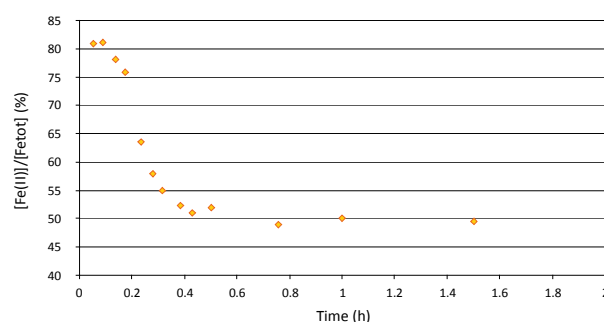


Figure 2. Time evolution of dissolved iron redox speciation during dissolution experiment on UP matter.

3. Simulation of a Cloud Event—Analysis of the Effect of Iron Dissolution on Cloud Chemistry

3.1. Model description and initialization

The M2C2 model is composed of two modules which can be coupled together: (1) a multiphase chemistry model (Leriche et al., 2000; Leriche et al., 2003; Deguillaume et al., 2004) and (2) a two-moment warm microphysical scheme module predicting the number concentration of cloud droplets and raindrops and the mixing ratio of cloud water and rainwater categories (Caro et al., 2004). The microphysical module has been recently expanded to consider the process of cloud droplet nucleation (Leriche et al., 2007) and the ice phase formation together with its effect on the budget of trace gases via retention and burial processes (Long et al., 2010). The dynamical framework of the model is an air parcel (Jeremy et al., 2000). The exchange of chemical species between the gas-phase and the aqueous-phase is parameterized following the mass transfer kinetic formulation developed by Schwartz (1986).

For the aqueous-phase (cloud and rainwater), the detailed chemistry of HO_x, chlorine, carbonates, NO_y, sulfur, the oxidation of organic volatile compounds (VOCs) with two carbon atoms, the chemistry of transition metal ions for iron, manganese and copper was included (Deguillaume et al., 2004). Table S1 to S7 summarizes the chemical reactions that were considered in the atmospheric aqueous-phase in the model for the simulations (see the Supporting Material, SM). The pH can also be calculated by solving the electro-neutrality equation. Photolysis frequencies in the gas-phase and in cloud droplets were calculated for 15 minute intervals using the Tropospheric Ultra-violet Model (TUV) (Madronich and Flocke, 1999).

An idealistic stable cloud event characterized by simplified microphysics was simulated. In this study, we did not consider complex microphysical processes (rain formation and interactions with aerosol particles), because the objective was to evaluate the influence of dissolution on the aqueous chemistry only. The liquid water content (0.3 g m^{-3}), the temperature (288.15 K), the pressure (1 000 hPa) and the droplet radius (10 μm) were set constant during the simulation, which lasted 2h. Throughout the simulation, the pH was held at 4.7, corresponding to the value used for the dissolution experiment (see Section 2). A chemical continental scenario was applied with initial concentrations of aqueous species adapted from Ervens et al. (2003) and previously used in Deguillaume et al. (2004) (Table 2). The initial gas-phase concentrations were similar to the rural scenario from Ervens et al. (2003) and are listed in Table S8 (see the SM). Two simulations were performed: (1) No dissolution process for iron is considered (Without dissolution). The iron concentrations were initialized with the iron concentration measured after 2 hours in the dissolution experiments, i.e. $1.7 \times 10^{-6} \text{ M}$ and assuming a speciation of $[\text{Fe(II)}]/[\text{Fe(III)}]$ equal to 4; (2) Dissolution kinetics were considered (With dissolution). In this case, dissolution kinetics were parameterized in the model following the two reactions described in Section 2.1, representing the labile and refractory iron phase dissolution steps for UP matter with kinetic data and iron redox speciation summarized in Table 1. These two steps are considered one after the other in the model: the second dissolution kinetic is considered only when R_1 is lower than R_2 .

Table 2. Initial aqueous-phase concentrations (adapted from Ervens et al., 2003)

Chemical species	Concentration (mol L^{-1})	
	Without dissolution	With dissolution
O ₂	3×10^{-4}	
Cl ⁻	1×10^{-4}	
HSO ₄ /SO ₄ ²⁻	6×10^{-5}	
Fe(III)	3.35×10^{-7}	X
Fe(II)	1.34×10^{-6}	X

3.2. Results and discussion on the cloud chemistry

The comparison between the simulations with and without dissolution kinetics will be discussed in terms of interactions of iron with H_xO_y chemistry which drives the oxidant capacity of the aqueous-phase. To illustrate this, Figure S1 (in the SM) reproduces the major chemistry pathways of H_xO_y radicals in the gas and aqueous-phases (adapted from Jacob, 2000). The case without dissolution has been discussed in Deguillaume et al. (2004) and the main conclusions are briefly recalled here. The production of OH radicals is mainly due to photolysis of Fe(III) following the Fenton reaction [between H₂O₂ and Fe(II)]. The oxidation of organics is the most important sink for the OH radical followed by its reactions with Fe(II), sulfite ions and hydrogen peroxide. The production of HO₂/O₂⁻ radicals is the result of the reaction of organics and H₂O₂ with OH radicals and the mass transfer from the gas-phase. Their destruction is mainly due to their reaction with Fe(III). The iron

redox speciation is determined by the balance between the Fenton reaction, the photolysis of Fe(III) and the reaction of Fe(III) with HO₂/O₂⁻.

For both runs, Figure 3 shows the time evolution of the total dissolved iron (3a), the iron redox concentrations (Fe(II) and Fe(III)) (3b) and the dissolved iron redox speciation (3c). In this work, the term “speciation” refers to the distinction between the various oxidation states of a chemical element and corresponds specifically to the ratio between the concentration of iron in its oxidation state (+II) and the concentration of dissolved iron.

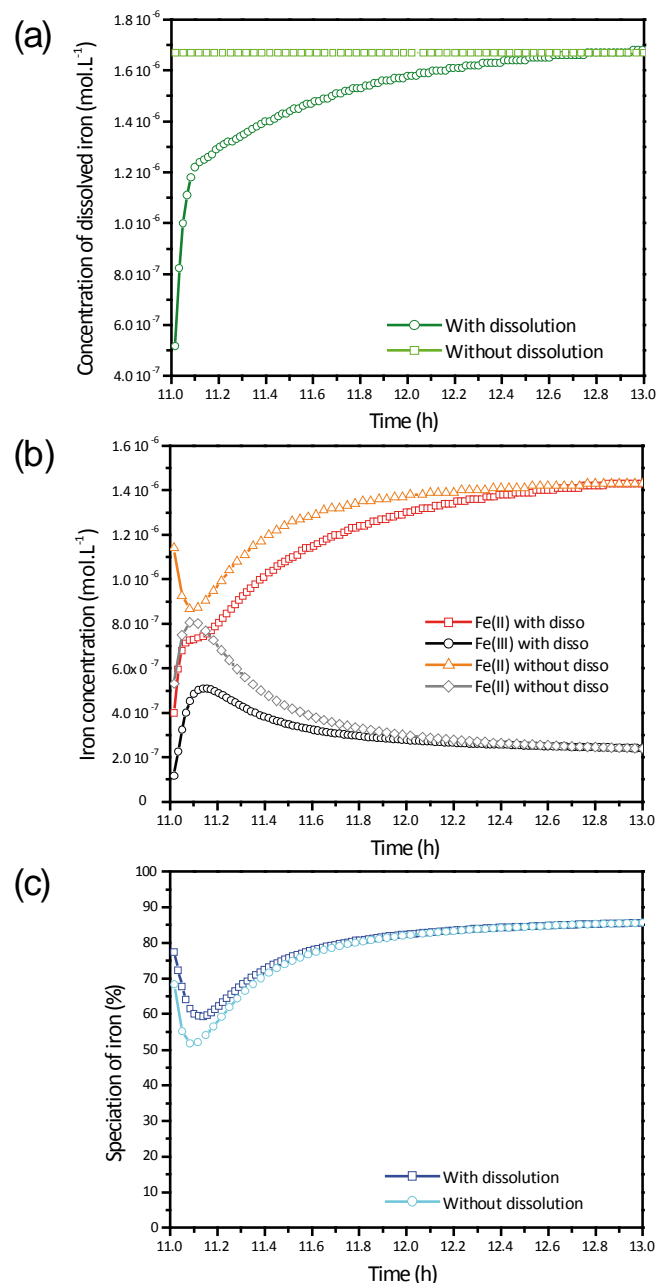


Figure 3. Time evolution of dissolved iron concentrations (a), of the major iron chemical species (Fe(II) and Fe(III)) (b), and speciation of dissolved iron ($[\text{Fe(II)}]/([\text{Fe(II)} + \text{Fe(III)}])$) in % (c) for the two scenarios: with and without dissolution of iron.

Finally, Table 3 summarizes the ratio of concentrations of iron and HO_x chemical species with dissolution over those without dissolution at different simulation times. For the simulation with dissolution, the iron content increases during the entire duration of the simulation approaching the constant value used in the case without dissolution at the end of the simulation (Figure 3a). The

increase of iron content is very rapid in the first 10 minutes of simulation, due to the high initial dissolution rate observed experimentally. Thus, after 10 minutes of simulation the dissolved iron content in the dissolution scenario represents 77% of the constant iron content (simulation without dissolution) and 94% after 1 hour (see Table 3). The time evolution of the iron speciation (Figure 3c) is similar in both simulations but, in the case with dissolution, the iron speciation is shifted towards higher values with a maximum of difference around 5 minutes after the beginning of the simulation where the iron speciation is 1.2 higher. When dissolution is considered, the input of Fe(II) by dissolution is controlled by Reaction (1) in the first 5 minutes, with a Fe(II)/Fe(III) ratio equal to 80/20, and then by Reaction (2) where the Fe(II)/Fe(III) ratio is 50/50. Figure 3c shows that in the case with dissolution, the contribution of Fe(II) is always superior to 50%, even when reaction (2) controls the dissolved iron release. Moreover, the main conversion pathways between Fe(II) and Fe(III) are identical in the two simulations (except for the dissolution sources pFe1 and pFe2). Thus, the general evolution of the iron redox speciation is mainly driven by the chemical reactivity and not by the dissolution process. This is confirmed by sensitivity tests on the initial speciation in Reactions of dissolution (1) and (2) which demonstrate a negligible impact on the temporal evolution of the iron redox speciation (not shown). These results show that the dissolution process is critical in simulating the iron concentrations, but is not critical in estimating the iron redox speciation in cloud droplets. This important point is consistent with some experimental results showing that the H_2O_2 concentrations or photolytic activity, for example, are the critical parameters that control the iron speciation (e.g. Marinoni et al., 2004; Majestic et al., 2007).

The H_xO_y chemistry is dependent on iron content and speciation in cloud droplets (Ervens et al., 2003; Deguillaume et al., 2004; Tilgner, 2009). Indeed, the time evolution of OH concentrations is significantly different between the two simulations

especially during the first hour of simulation (Figure 4). Initially, in the case with dissolution, OH concentration is 2.8 times smaller than the case without dissolution and the concentration increases by a factor of 1.45 in 30 minutes (from 2.4×10^{-13} to $3.5 \times 10^{-13} \text{ mol L}^{-1}$). This is due to the continuous transfer of Fe(III) in cloud water by dissolution which is photolyzed and produces OH radicals. However, as soon as the difference on the iron content is inferior to 25% between the two scenarios, i.e. at 30 minutes simulation time, the OH radical concentration ratio reaches 90% of the concentrations simulated in the scenario without dissolution (Table 3). This means that the indirect dissolution effect on iron concentration appears negligible in comparison to chemical process of OH production. The OH ratios are similar to the Fe(II) ratios, this shows the importance of the photolysis of Fe(III) into Fe(II) in the production of OH. The time series of the HO_2/O_2^- ratio is also modified: without dissolution of iron, HO_2/O_2^- radicals react immediately with Fe(III) in excess, whereas when Fe(III) is continuously introduced into the aqueous-phase, HO_2/O_2^- is less efficiently consumed. Similarly to iron, the concentrations of radicals are equal after two hours of simulation in both simulations, indicating that iron concentrations control radical concentrations.

To get into more details, Figure 5 illustrates the relative contribution of the sources and sinks of the OH radical in the aqueous-phase over the cloud period and thereby the interactions of the OH radical with the iron redox cycling. Without dissolution, the initial fluxes of OH production and destruction are intense, since the iron concentrations are initially fixed and values of these fluxes decrease throughout the simulation. Dissolution tends to reduce sink and source fluxes of OH radicals in cloud droplets during the first 30 minutes. At the end of the simulation, we observed the same chemical regime of OH radicals than in the case without dissolution.

Table 3. Ratio of iron [total iron, Fe(II), Fe(III) and iron speciation] and HO_x concentrations (OH and HO_2/O_2^- radicals) with dissolution over those without dissolution for various times of simulation ("D": with dissolution and "WD": without dissolution)

Time of simulation (minutes)	$[\text{Fe}_{\text{tot}}]_{\text{D}}/[\text{Fe}_{\text{tot}}]_{\text{WD}}$	$[\text{Fe(II)}]_{\text{D}}/[\text{Fe(II)}]_{\text{WD}}$	$[\text{Fe(III)}]_{\text{D}}/[\text{Fe(III)}]_{\text{WD}}$	$[\text{Fe(II)}]/([\text{Fe(II)}]+[\text{Fe(III)}])_{\text{D}}/([\text{Fe(II)}]+[\text{Fe(III)}])_{\text{WD}}$	$[\text{OH}]_{\text{D}}/[\text{OH}]_{\text{WD}}$	$[\text{HO}_2]_{\text{D}}/[\text{HO}_2]_{\text{WD}}$
5	0.73	0.81	0.60	1.20	0.78	1.38
10	0.77	0.82	0.69	1.08	0.82	1.24
15	0.92	0.83	0.73	1.04	0.85	1.20
20	0.82	0.84	0.77	1.03	0.88	1.17
30	0.86	0.87	0.82	1.02	0.91	1.13
40	0.90	0.90	0.86	1.01	0.94	1.10
50	0.92	0.92	0.90	1.01	0.95	1.07
60	0.94	0.94	0.92	1.00	0.97	1.06
90	0.98	0.98	0.97	1.00	0.99	1.02
120	1.00	1.00	1.00	1.00	1.00	1.00

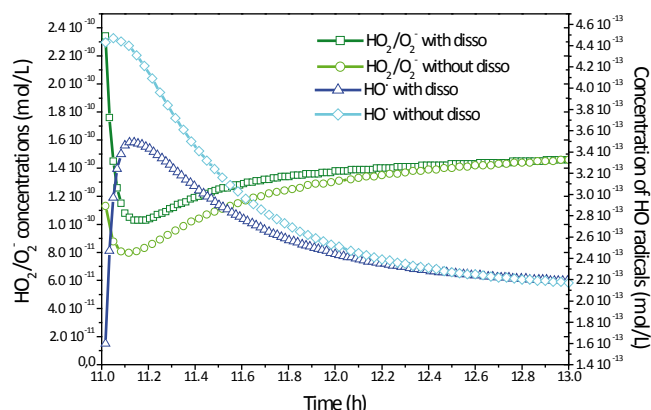


Figure 4. Time evolution of HO_x concentrations (OH and HO_2/O_2^- radicals) simulated with the M2C2 model for the 2 cases: with and without dissolution of iron.

These results demonstrate that during the first 30 minutes of the cloud simulation, the chemistry is modified by the kinetic of iron dissolution, which leads to a decrease in the oxidizing capacity of the cloud water. On the other hand, after 2 hours of the simulation, the concentrations of iron and radicals are not significantly modified. Thus, the total iron content in the cloud droplet is a key factor that controls the oxidative property of the

cloud water. It will control the HO_x chemistry in the simulation and therefore the ability of the aqueous-phase chemistry to transform pollutants such as organics and sulfite. When the iron concentrations are initially fixed, the global OH radical concentration is overestimated during the first 30 minutes of the simulation. To quantify this effect, Table 4(a) includes the production and destruction of OH radicals by iron chemical pathways integrated over several simulation times for the two scenarios, as well as the resulting net production. When dissolution is activated, the net production of OH radicals by iron reactions in the aqueous-phase decreases respectively from 41% after 5 minutes of simulation time to 17% over 2 hours of simulation (Table 4b). This confirms a significant overestimation of aqueous concentration of OH radicals. Consequently, the gas-phase concentration of OH radicals is also overestimated when dissolution process is not activated (7% and 11% of enhancement of the gas-phase OH radical production respectively integrated over the first 30 minutes and 2 hours of simulation). Indeed, in the case with dissolution, an efficient transfer of gaseous OH radicals in the aqueous-phase is observed over the first 30 minutes and the reverse in the case without dissolution over the whole duration of the simulation. This results demonstrate the time dependency of the mass transfer processes towards the over and/or underestimation of OH radicals production in the aqueous-phase.

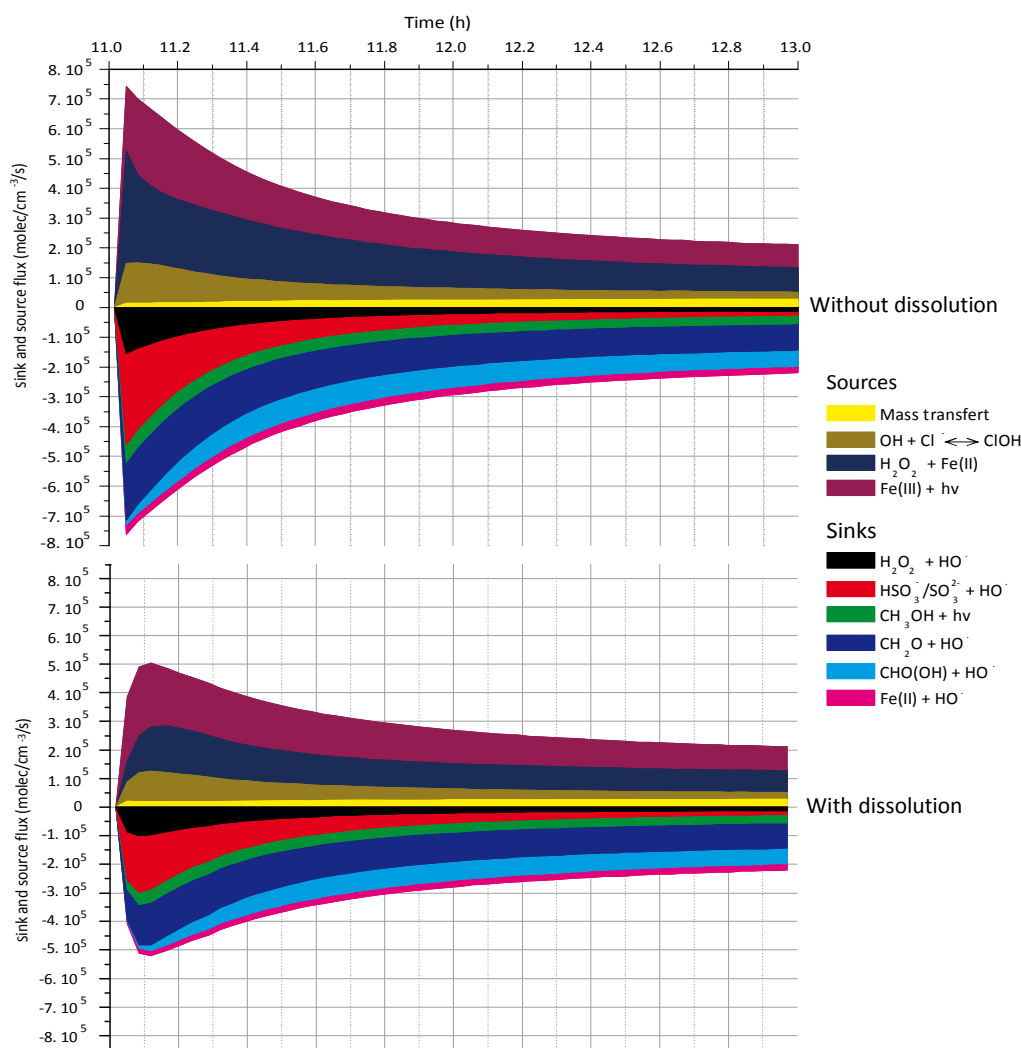


Figure 5. Time evolution of sources and sinks of OH radicals over the cloud period for the two cases: with and without dissolution of iron.

Table 4. (a) Production and destruction of aqueous OH radicals by reactions with iron (in molec cm⁻³) integrated over different simulation times and the resulting net production ("TOT"); **(b)** Relative decrease of OH radicals production due to dissolution of iron for several simulation times (in %)

(a)	Production (molec cm ⁻³)		Destruction (molec cm ⁻³)		Total net Production (molec cm ⁻³) "TOT"	
	Fe(III) + hv Fe(II) + H ₂ O ₂		Fe(II) + OH			
Simulation time (minutes)	With dissolution	Without dissolution	With dissolution	Without dissolution	With dissolution	Without dissolution
5	8.02 × 10 ⁷	1.38 × 10 ⁸	3.32 × 10 ⁶	7.41 × 10 ⁶	7.69 × 10 ⁷	1.31 × 10 ⁸
10	1.69 × 10 ⁸	2.60 × 10 ⁸	7.85 × 10 ⁶	1.42 × 10 ⁷	1.61 × 10 ⁸	2.46 × 10 ⁸
20	3.30 × 10 ⁸	5.22 × 10 ⁸	1.79 × 10 ⁷	3.20 × 10 ⁷	3.12 × 10 ⁸	4.90 × 10 ⁸
30	5.04 × 10 ⁸	7.34 × 10 ⁸	3.15 × 10 ⁷	5.00 × 10 ⁷	4.73 × 10 ⁸	6.84 × 10 ⁸
60	9.09 × 10 ⁸	1.20 × 10 ⁹	7.32 × 10 ⁷	9.89 × 10 ⁷	8.36 × 10 ⁸	1.10 × 10 ⁹
120	1.54 × 10 ⁹	1.85 × 10 ⁹	1.52 × 10 ⁸	1.84 × 10 ⁸	1.39 × 10 ⁹	1.67 × 10 ⁹

(b)	5 min	10 min	20 min	30 min	60 min	120 min
(TOT without dissolution – TOT with dissolution)/TOT without dissolution	41%	36%	36%	30%	24%	17%

These results have been obtained in the framework of a model scenario considering a 2-h persistent cloud with a constant cloud droplet diameter and constant liquid water content. However, in real clouds, cloud droplet lifetime typically ranges from a few minutes to 30 minutes depending on the cloud type (Colville et al., 1997; Pruppacher and Klett, 1997). As the effect of the kinetics of iron dissolution on cloud chemistry are mainly significant during the first 30 minutes of the simulation time, one can expect a significant effect on real cloud through a decrease of the oxidizing capacity of the cloudy atmosphere. Indeed, for instance, a decrease of the production of sulfate and secondary organic compounds is expected. In our academic simulation, considering dissolution leads to 15% less sulfate concentration after 30 minutes of simulation. For organics, only C1 oxidation is considered in the model and, even if a decrease in formic acid concentration together with an increase in formaldehyde concentration is observed when dissolution is considered, the difference is not very significant. However, it is difficult to generalize these results to complex cloud organic chemistry.

It is rather difficult to compare our results with *in situ* measurements since we consider an idealistic scenario where the dissolution kinetics can be taken into account. *In situ* measurements of iron concentrations and speciation in cloud water show great heterogeneity since they depend on many environmental parameters such as meteorological conditions, air mass origin, primary emissions and droplet properties (Deguillaume et al., 2005b). Moreover, due to the sampling duration, the information relative to the dissolution processes cannot be reached by *in situ* measurements.

4. Conclusion

To understand the impact of iron on atmospheric chemistry, chemical and dissolution kinetics need to be considered together in cloud chemistry models to assess their relative contributions. The incorporation of iron dissolution kinetics from laboratory studies in the M2C2 model showed that this process is essential to obtain more realistic concentrations of dissolved iron in cloud droplets, especially during the first 30 minutes of the simulation. The results demonstrated that dissolution is not the driving process controlling dissolved iron redox speciation in the clouds, but is essential to simulate the amount of dissolved iron and thus,

the cloud chemical reactivity. The concentration of iron governs the concentration of radicals in cloud droplet, but also partly in the gaseous phase (due to the rate of the mass transfer). Ignoring the dissolution kinetics of iron results in an overestimation of OH net production, by a factor of 1.7 after 5 minutes and a factor of 1.2 after 2 hours of simulation time, respectively.

The consideration of the dissolution process is potentially important in estimating radical concentrations and hence cloud oxidative capacity. Presently, dissolution kinetic processes are not included in cloud chemistry models. On the other hand, iron dissolution rates are used in biogeochemical models to estimate iron fluxes to the ocean, notably via hematite dissolution (e.g. Meskhidze et al., 2005; Baker and Croot, 2010; Mahowald et al., 2005). A recent publication (Journet et al., 2008) indicates that besides hematite, dissolved iron mainly comes from clay dissolution. This finding confirms that iron solubility is closely linked to the mineralogical composition of the aerosol. In the future, investigations on the dissolution of iron, but also of other transition metals (i.e., copper and manganese) from aerosols of various origins or minerals should be carried out to enable a better estimation of the oxidative capacity of atmosphere. Indeed, the coexistence of catalytically active transition metals in atmospheric liquid water exhibits synergy on cloud chemistry (sulfur, H₂O₂, and oxidation of organics). The assessment of the concentrations of dissolved metal is complex and requires a significant effort to parameterize the effect of each factor. For example, the gradient in pH and ionic strength sustained by aerosol during cloud processes needs to be considered during laboratory investigations as well as organic ligands and biological activities that will act to enhance solubility of metals. In this article, our investigation is limited to rather simple model calculations designed to determine the effect of dissolution on cloud chemistry to mimic laboratory simulations. Finally, this study demonstrates that the cloud chemical model is a complementary tool for laboratory investigations which helps to interpret the experimental results and to apply them into real atmospheric conditions (temperature, variable LWC, polydisperse cloud etc.).

Acknowledgements

This work was supported by the Programme National de Chimie Atmosphérique (PNCA) of the Institut des Sciences de

l'Univers (INSU). We gratefully acknowledge Pascal Bleuyard for his invaluable computer support. The first author is very grateful to Jamila Bardouki, Marie Camredon, Nickolas Good, Emilie Journet and Florence Holop for their useful comments.

Supporting material available

Figure S1 describes the main chemistry pathways of H_xO_y radicals in the aqueous-phase and in the gas-phase and their coupling. Tables S1 to S7 list the chemical reactions in the aqueous-phase that are considered in the M2C2 model. Table S8 summarizes the initial gaseous concentrations for the two simulations (with and without dissolution). This information is available free of charge via the Internet at <http://www.atmospolres.com>.

References

- Alexander, B., Park, R.J., Jacob, D.J., Gong, S., 2009. Transition metal-catalyzed oxidation of atmospheric sulfur: global implications for the sulfur budget. *Journal of Geophysical Research D: Atmospheres* 114, art.no.D02309.
- Baker, A.R., Croot, P.L., 2010. Atmospheric and marine controls on aerosol iron solubility in seawater. *Marine Chemistry* 120, 4-13.
- Barth, M.C., 2006. The importance of cloud drop representation on cloud photochemistry. *Atmospheric Research* 82, 294-309.
- Biscombe, A., Nimmo, M., Gledhill, M., Achterberg, E.P., 2004. An automated monitor to determine trace metal particle/dissolved interactions in natural waters. *Analytica Chimica Acta* 521, 69-76.
- Caro, D., Wobrock, W., Flossmann, A.I., Chaumerliac, N., 2004. A two-moment parameterization of aerosol nucleation and impaction scavenging for a warm cloud microphysics: description and results from a two-dimensional simulation. *Atmospheric Research* 70, 171-208.
- Chester, R., Murphy, K.J.T., Lin, F.J., Berry, A.S., Bradshaw, G.A., Corcoran, P.A., 1993. Factors controlling the solubilities of trace metals from non-remote aerosols deposited to the sea surface by the 'dry' deposition mode. *Marine Chemistry* 42, 107-126.
- Colville, R.N., Bower, K.N., Choularton, T.W., Gallagher, M.W., Beswick, K.M., Arends, B.G., Kos, G.P.A., Wobrock, W., Schell, D., Hargreaves, K.J., Storeton-West, R.L., Cape, J.N., Jones, B.M.R., Wiedensohler, A., Hansson, H.C., Wendisch, M., Acker, K., Wiprecht, W., Pahl, S., Winkler, P., Berner, A., Krusis, C., Gieray, R., 1997. Meteorology of the great dun fell cloud experiment 1993. *Atmospheric Environment* 31, 2407-2420.
- Deguillaume, L., Leriche, M., Chaumerliac, N., 2005a. Impact of radical versus non-radical pathway in the Fenton chemistry on the iron redox cycle in clouds. *Chemosphere* 60, 718-724.
- Deguillaume, L., Leriche, M., Monod, A., Chaumerliac, N., 2004. The role of transition metal ions on HO_x radicals in clouds: a numerical evaluation of its impact on multiphase chemistry. *Atmospheric Chemistry and Physics* 4, 95-110.
- Deguillaume, L., Leriche, M., Desboeufs, K., Mailhot, G., George, C., Chaumerliac, N., 2005b. Transition metals in atmospheric liquid phases: sources, reactivity, and sensitive parameters. *Chemical Reviews* 105, 3388-3431.
- Desboeufs, K.V., Losno, R., Colin, J.L., 2001. Factors influencing aerosol solubility during cloud processes. *Atmospheric Environment* 35, 3529-3537.
- Desboeufs, K.V., Losno, R., Colin, J.L., 2003a. Figures of merit of pneumatic and ultrasonic sample introduction systems in inductively coupled plasma-multichannel-based emission spectrometry in an ultra-clean environment. *Analytical and Bioanalytical Chemistry* 375, 567-573.
- Desboeufs, K.V., Losno, R., Colin, J.L., 2003b. Relationship between droplet pH and aerosol dissolution kinetics: effects of incorporated aerosol particles on droplet pH during cloud processing. *Journal of Atmospheric Chemistry* 46, 159-172.
- Desboeufs, K.V., Losno, R., Vimeux, F., Cholbi, S., 1999. The pH-dependent dissolution of wind-transported Saharan dust. *Journal of Geophysical Research* 104, 21287-21299.
- Desboeufs, K.V., Sofikitis, A., Losno, R., Colin, J.L., Ausset, P., 2005. Dissolution and solubility of trace metals from natural and anthropogenic aerosol particulate matter. *Chemosphere* 58, 195-203.
- Erel, Y., Pehkonen, S.O., Hoffmann, M.R., 1993. Redox chemistry of iron in fog and stratus clouds. *Journal of Geophysical Research* 98, 18423-18434.
- Ervens, B., Carlton, A.G., Turpin, B.J., Altieri, K.E., Kreidenweis, S.M., Feingold, G., 2008. Secondary organic aerosol yields from cloud-processing of isoprene oxidation products. *Geophysical Research Letters* 35, art. no. L02816.
- Ervens, B., George, C., Williams, J.E., Buxton, G.V., Salmon, G.A., Bydder, M., Wilkinson, F., Dentener, F., Mirabel, P., Wolke, R., Herrmann, H., 2003. CAPRAM 2.4 (MODAC mechanism): an extended and condensed tropospheric aqueous phase mechanism and its application. *Journal of Geophysical Research D: Atmospheres* 108, AAC 12-1 - AAC 12-21.
- Fowler, D., Pilegaard, K., Sutton, M.A., Ambus, P., Raivonen, M., Duyzer, J., Simpson, D., Fagerli, H., Fuzzi, S., Schjoerring, J.K., Granier, C., Neftel, A., Isaksen, I.S.A., Laj, P., Maione, M., Monks, P.S., Burkhardt, J., Daemmgen, U., Neiryneck, J., Personne, E., Wichink-Kruit, R., Butterbach-Bahl, K., Flechard, C., Tuovinen, J.P., Coyle, M., Gerosa, G., Loubet, B., Altimir, N., Gruenhage, L., Ammann, C., Cieslik, S., Paoletti, E., Mikkelsen, T.N., Ro-Poulsen, H., Cellier, P., Cape, J.N., Horvath, L., Loreto, F., Niinemets, U., Palmer, P.I., Rinne, J., Misztal, P., Nemitz, E., Nilsson, D., Pryor, S., Gallagher, M.W., Vesala, T., Skiba, U., Brüggemann, N., Zechmeister-Boltenstern, S., Williams, J., O'Dowd, C., Facchini, M.C., de Leeuw, G., Flossman, A., Chaumerliac, N., Erisman, J.W., 2009. Atmospheric composition change: ecosystems-atmosphere interactions. *Atmospheric Environment* 43, 5193-5267.
- Gelencser, A., Varga, Z., 2005. Evaluation of the atmospheric significance of multiphase reactions in atmospheric secondary organic aerosol formation. *Atmospheric Chemistry and Physics* 5, 2823-2831.
- Jeremy, G., Wobrock, W., Flossmann, A.I., Schwarzenboeck, A., Mertes, S., 2000. A modelling study on the activation of small Aitken-mode aerosol particles during CIME 97. *Tellus, Series B: Chemical and Physical Meteorology* 52, 959-979.
- Hand, J.L., Mahowald, N.M., Chen, Y., Siefert, R.L., Luo, C., Subramaniam, A., Fung, I., 2004. Estimates of atmospheric-processed soluble iron from observations and a global mineral aerosol model: biogeochemical implications. *Journal of Geophysical Research D: Atmospheres* 109, art. no. D17205.
- Herrmann, H., Tilgner, A., Barzaghi, P., Majdik, Z., Gligorovski, S., Poulain, L., Monod, A., 2005. Towards a more detailed description of tropospheric aqueous phase organic chemistry: CAPRAM 3.0. *Atmospheric Environment* 39, 4351-4363.
- Herrmann, H., 2003. Kinetics of aqueous phase reactions relevant for atmospheric chemistry. *Chemical Reviews* 103, 4691-4716.
- Hoffmann, P., Dedik, A.N., Deutsch, F., Sinner, T., Weber, S., Eichler, R., Sterkel, S., Sastri, C.S., Ortner, H.M., 1997. Solubility of single chemical compounds from an atmospheric aerosol in pure water. *Atmospheric Environment* 31, 2777-2785.
- Jacob, D.J., 2000. Heterogeneous chemistry and tropospheric ozone. *Atmospheric Environment* 34, 2131-2159.
- Jickells, T.D., An, Z.S., Andersen, K.K., Baker, A.R., Bergametti, C., Brooks, N., Cao, J.J., Boyd, P.W., Duce, R.A., Hunter, K.A., Kawahata, H., Kubilay, N., LaRoche, J., Liss, P.S., Mahowald, N., Prospero, J.M., Ridgwell, A.J., Tegen, I., Torres, R., 2005. Global iron connections between desert dust, ocean biogeochemistry and climate. *Science* 208, 65-71.
- Journet, E., Desboeufs, K.V., Caqueneau, S., Colin, J.L., 2008. Mineralogy as a critical factor of dust iron solubility. *Geophysical Research Letters* 35, art. no. L07805.
- Journet, E., Desboeufs, K.V., Sofikitis, A., Varrault, G., Colin, J.L., 2007. In situ speciation of trace Fe(II) and Fe(III) in atmospheric waters by the

- FZ method coupled to GFAAS analysis. *International Journal of Environmental Analytical Chemistry* 87, 647-658.
- Leriche, M., Curier, R.L., Deguillaume, L., Caro, D., Sellegri, K., Chaumerliac, N., 2007. Numerical quantification of sources and phase partitioning of chemical species in cloud: application to wintertime anthropogenic air masses at the Puy de Dome station. *Journal of Atmospheric Chemistry* 57, 281-297.
- Leriche, M., Deguillaume, L., Chaumerliac, N., 2003. Modeling study of strong acids formation and partitioning in a polluted cloud during wintertime. *Journal of Geophysical Research D: Atmospheres* 108, AAC 14-1 - AAC 14-11.
- Leriche, M., Voisin, D., Chaumerliac, N., Monod, A., Aumont, B., 2000. A model for tropospheric multiphase chemistry: application to one cloudy event during the CIME experiment. *Atmospheric Environment* 34, 5015-5036.
- Li, Z., Aneja, V.P., 1992. Regional analysis of cloud chemistry at high elevations in the eastern United States. *Atmospheric Environment Part A. General Topics* 26, 2001-2017.
- Long, Y., Chaumerliac, N., Deguillaume, L., Leriche, M., Champeau, F., 2010. Effect of mixed-phase cloud on the chemical budget of trace gases: a modeling approach. *Atmospheric Research* 97, 540-554.
- Mackie, D.S., Boyd, P.W., Hunter, K.A., McTainsh, G.H., 2005. Simulating the cloud processing of iron in Australian dust: pH and dust concentration. *Geophysical Research Letters* 32, art. no. L06809.
- Madronich, S., Flocke, S., 1999. *The Role of Solar Radiation in Atmospheric Chemistry*. Handbook of Environmental Chemistry, Springer-Verlag, pp. 1-26.
- Mahowald, N.M., Baker, A.R., Bergametti, G., Brooks, N., Duce, R.A., Jickells, T.D., Kubilay, N., Prospero, J.M., Tegen, I., 2005. Atmospheric global dust cycle and iron inputs to the ocean. *Global Biogeochemical Cycles* 19, art. no. GB4025.
- Majestic, B.J., Schauer, J.J., Shafer, M.M., 2007. Application of synchrotron radiation for measurement of iron red-ox speciation in atmospherically processed aerosols. *Atmospheric Chemistry and Physics* 7, 2475-2487.
- Marinoni, A., Laj, P., Sellegri, K., Mailhot, G., 2004. Cloud chemistry at the Puy de Dôme: variability and relationships with environmental factors. *Atmospheric Chemistry and Physics* 4, 715-728.
- Medina, J., Nenes, A., 2004. Effects of film-forming compounds on the growth of giant cloud condensation nuclei: implications for cloud microphysics and the aerosol indirect effect. *Journal of Geophysical Research D: Atmospheres* 109, art. no. D20207.
- Meskhidze, N., Chameides, W.L., Nenes, A., 2005. Dust and pollution: a recipe for enhanced ocean fertilization? *Journal Geophysical Research D: Atmospheres* 110, art. no. D03301.
- Nimmo, M., Fones, G.R., Chester, R., 1998. Atmospheric deposition: a potential source of trace metal organic complexing ligands to the marine environment. *Croatica Chemica Acta* 71, 323-341.
- Ozsoy, T., Saydam, A.C., 2001. Iron speciation in precipitation in the North-Eastern Mediterranean and its relationship with Sahara dust. *Journal of Atmospheric Chemistry* 40, 41-76.
- Parazols, M., Marinoni, A., Amato, P., Abida, O., Laj, P., Mailhot, G., 2006. Speciation and role of iron in cloud droplets at the puy de Dome station. *Journal of Atmospheric Chemistry* 54, 267-281.
- Pruppacher, H.R., Klett, J.D., 1997. *Microphysics of clouds and precipitation*. Kluwer Academics Publishers, 954 pp.
- Ridame, C., Guieu, C., 2002. Saharan input of phosphorus to the oligotrophic water of the open western Mediterranean. *Limnology and Oceanography* 47, 856-869.
- Schwartz, S.E., 1986. *Mass-Transport Considerations Pertinent to Aqueous Phase Reactions of Gases in Liquid-Water Clouds*. Vol. G6, Chemistry of Multiphase Atmospheric Systems, Springer, pp. 415-471.
- Sehili, A.M., Wolke, R., Helmert, J., Simmel, M., Schroder, W., Renner, E., 2007. Cloud Chemistry Modeling: Parcel and 3D Simulations. *Air Pollution Modeling and Its Application XVII*, 340-350 pp.
- Sinner, T., Hoffmann, P., Ortner, H.M., 1994. Determination of pH-value, redox- potential, transition metals concentration and Fe(II)- and Fe(III)- content in cloud water samples. *Contributions to Atmospheric Physics* 67, 353-357.
- Sofikitis, A.M., Colin, J.L., Desboeufs, K.V., Losno, R., 2004. Iron analysis in atmospheric water samples by atomic absorption spectroscopy (AAS) in water-methanol. *Analytical and Bioanalytical Chemistry* 378, 460-464.
- Spokes, L.J., Jickells, T.D., 1996. Factors controlling the solubility of aerosol trace metals in the atmosphere and on mixing into seawater. *Aquatic Geochemistry* 1, 355-374.
- Spokes, L.J., Jickells, T.D., Lim, B., 1994. Solubilisation of aerosol trace metals by cloud processing: a laboratory study. *Geochimica et Cosmochimica Acta* 58, 3281-3287.
- Stumm, W., Morgan, J.J., 1996. *Aquatic Chemistry : Chemical Equilibria and Rates in Natural Waters*. 3rd ed. Wiley, pp. 252-348.
- Tilgner, A., 2009. Modelling of the physico-chemical multiphase processing of tropospheric aerosols, IfT, Fakultät für Physik und Geowissenschaften.
- Tilgner, A., Majdik, Z., Sehili, A.M., Simmel, M., Wolke, R., Herrmann, H., 2005. SPACCIM: Simulations of the multiphase chemistry occurring in the FEBUKO hill cap cloud experiments. *Atmospheric Environment* 39, 4389-4401.
- Von Glasow, R., Lawrence, M.G., Sander, R., Crutzen, P.J., 2003. Modeling the chemical effects of ship exhaust in the cloud-free marine boundary layer. *Atmospheric Chemistry and Physics* 3, 233-250.
- Wolke, R., Sehili, A.M., Simmel, M., Knoth, O., Tilgner, A., Herrmann, H., 2005. SPACCIM: A parcel model with detailed microphysics and complex multiphase chemistry. *Atmospheric Environment* 39, 4375-4388.
- Zuo, Y., 1995. Kinetics of photochemical/chemical cycling of iron coupled with organic substances in cloud and fog droplets. *Geochimica et Cosmochimica Acta* 59, 3123-3130.